AC Resistance Considering the Magnetic Saturation in the Motor

Ho-Young Lee, Kyu-Seob Kim, and Jung-Pyo Hong

Department of Automotive Engineering, Hanyang University, Seoul 133-791, Republic of Korea

According to the trend of the decreasing size of electric machines, the winding techniques for maximizing the space factor have been studied of late in an effort to improve the power density, but such techniques have been found to worsen the eddy current effect, which is caused by the alternating current in the conductor. Therefore, the introduction of the AC resistance needed for the exacted motor performance prediction since the AC resistance loss, which has been ignored, has gradually increased. In the case of the conductor surrounded by the ferromagnetic material, the eddy current effect is dependent not only on the frequency but also on the magnetic saturation in the core. The analytic AC resistance for the slot-bound conductor has been reported, but it does not consider the magnetic saturation in the core. This paper presents the analytic equation considering the magnetic saturation in the core. Also, the EI core, which is identical to the motor shape, was manufactured to verify the reliability of the analytical equation, and was experimented on. As a result, the result of the presented equation has an identical tendency with the test and FEM results.

***Index Terms* — Copper loss, core loss, eddy current, proximity effect, skin effect**

I. Introduction

THE AUTOMOTIVE application demands the motor to characterize the high-efficiency and wide-speed operation. Above all things, the miniaturization of the motor is important due to the space restriction and weight. According to the need for miniaturization, the winding techniques for maximizing the space factor have been studied in an effort to improve the power density [1], but such techniques have been found to worsen the eddy current effect, which is caused by the alternating current in the conductor.

It is well known that the presence of a magnetic field within a conductor produces eddy current, and that this current induces a magnetic field, which attempts to cancel the applied field. When the applied magnetic field is due itself to the conductor current, this phenomenon is called skin effect, and if the magnetic field is due to a source outside the conductor, such phenomenon is called proximity effect.

In the case where the conductor is surrounded by a ferromagnetic material, the eddy current more remarkably occurs because much of the flux induced by the alternating current passes through the dense ferromagnetic material [2]. Therefore, this phenomenon varies with the degree of magnetic saturation of the core.

The analytic AC resistance for the slot-bound conductor has been reported, but it does not consider the magnetic saturation in the core. This paper provides the analytical equation for the AC resistance considering the magnetic saturation of the core to perform the loss prediction of the motor's high reliability. This paper presents the saturation factor based on the assumptions shown below.

(a) The entire motor winding and end turn is not considered.
(b) This paper handles the insulated rectangular conduct.
(c) The leakage flux lines across the slot rectilinearly.
(d) The permeability of iron is infinite.

The presented saturation factor complemented the equation of the exciting AC resistance. Furthermore, the EI core, which is identical to the motor shape, was manufactured to verify the reliability of the analytical equation. The formula result was compared with the test and FEM results.

Manuscript received March 7, 2014. Corresponding author: Jung-Pyo Hong (e-mail: hongjp@hanyang.ac.kr).
Digital Object Identifier inserted by IEEE

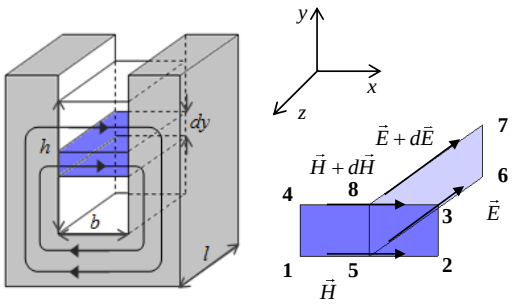

Fig. 1. Solid conductor in a slot surrounded on three sides by the core.

II. Analytical Theory

A. AC Resistance Expressions to the Slot-bound Conductor

Consider a solid conductor in a slot surrounded on three sides by a ferromagnetic material [3]. The vector of the current density J and electric field strength E in the conductor have only a z-component. The magnetic field strength H and the flux density B have only an x-component across the conductor. Applying Ampere's law to route 1-2-3-4-1, the following equation is obtained:

$$\oint \vec{H}\cdot d\vec{l} = Hb - \left(H + \frac{\partial H}{\partial y}dy\right)b = Jbdy \tag{1}$$

from which

$$-\frac{\partial H}{\partial y} = J \tag{2}$$

Also, by applying Faraday's induction law to route 5-6-7-8-5 in Fig. 1, the following equation is obtained:

$$\oint \vec{E}\cdot d\vec{l} = -El + \left(E + \frac{\partial E}{\partial y}dy\right)l = -\frac{\partial B}{\partial t}ldy \tag{3}$$

from which

$$\frac{\partial E}{\partial y}=\frac{\partial B}{\partial y}=\mu_o\frac{\partial H}{\partial y}=-j\omega\mu_o H \tag{4}$$

From equation (2) with respect to y and using (4),

$$\frac{\partial^2 H_x(y)}{\partial y^2}=\frac{\partial J}{\partial y}=\sigma\frac{\partial E_z}{\partial y}=-j\sigma\mu_o\omega H_x(y)=j\frac{2}{\delta^2}H_x(y) \tag{5}$$

where $j=\sqrt{(-1)}$, $\delta=\sqrt{2/\sigma\mu\omega}$ is the skin depth of the material, ω is the frequency of excitation in radians per second, μ is the permeability of the conducting sheet, and σ is the sheet conductivity. The solution of equation (5) is

$$H_x(y)=\frac{H_a\sinh\alpha(h-y)+H_b\sinh\alpha y}{\sinh(\alpha h)} \tag{6}$$

where $\alpha=(1+j)/\delta$. Using $\nabla\times\vec{H}=\vec{J}$, the current density associated with this magnetic-field distribution has only a z-component, which is given by

$$J_z(y)=\frac{\alpha\{H_a\cosh\alpha(h-y)-H_b\cosh(\alpha y)\}}{\sinh(\alpha h)} \tag{7}$$

The average power dissipated in the conductor per square in the plane is

$$P_{\square}=\frac{1}{\sigma}\int_0^h J(y)J^*(y)\,\mathrm{d}y \tag{8}$$

where J^* is the complex conjugate of J. Substituting equation (7) into equation (8) and performing integration gives

$$P_{\square}=\frac{1}{\sigma h}\left\{(H_a-H_b)^2\Delta F(\Delta)+2H_aH_b\Delta G(\Delta)\right\} \tag{9}$$

where $\nabla=h/\delta$,

$$F(\Delta)=\frac{\sinh 2\Delta+\sin 2\Delta}{\cosh 2\Delta-\cos 2\Delta},\ \text{and}\ G(\Delta)=\frac{\sinh\Delta-\sin\Delta}{\cosh\Delta+\cos\Delta} \tag{10}$$

Consider the case shown in Fig. 2, where several conductors are placed in a slot [4]. All the conductors are series-connected. There are n_d conductors on top of each other, n_w adjacent conductors, and $n_s=n_d\cdot n_w$ total number of conductors.

The magnetic field at the top of the conductors in the nth row is

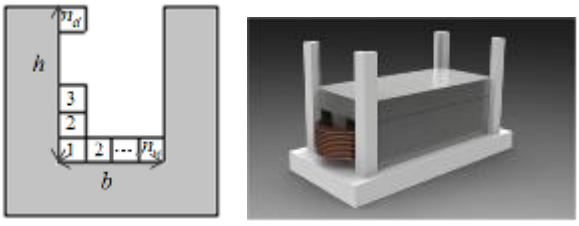

Fig. 2. Several conductors placed on the slot.

$$H_x(n)=H_x(y)=\frac{n_w I}{b}n,\ \text{and}\ n=0,1,...,n_d \tag{11}$$

where I is the current on each conductor. Therefore, the magnetic fields at the bottom and top of the nth row are

$$(H_a-H_b)^2=\{H_x(1)\}^2=H_1^2\ \text{and}\ H_aH_b=H_1^2n(n-1) \tag{12}$$

Substituting these expressions into equation (9) will give the power loss per square in a conductor in the nth row as

$$P_{\square}(n)=\frac{H_1^2}{\sigma h}\{\Delta F(\Delta)+2n(n-1)\Delta G(\Delta)\} \tag{13}$$

After multiplying equation (13) by the *y* and *z* dimensions and simplifying the result, the power loss in the conductors of the nth row are obtained respectively using the following equation:

$$P(n)=I^2R_cn_w\{\Delta F(\Delta)+2n(n-1)\Delta G(\Delta)\} \tag{14}$$

where $R_c=L_s/(\sigma\mathrm{h}^2)$ is the DC resistance of a single-slot conductor and L_s is the slot length. It is clear from equation (14) that the power loss increases as one moves from the slot bottom (n=1) to the slop (n=n_d). Thus, more heat and loss are generated at the slot top.

The total power loss in the slot is given by the sums of equation (15) over all the n_d rows.

$$P=I^2R_cn_s\left\{\Delta F(\Delta)+\frac{2}{3}(n_d^2-1)\Delta G(\Delta)\right\} \tag{15}$$

Total slot resistance R_{AC} gives [4]

$$R_{AC}=R_{dc}\left\{\Delta F(\Delta)+\frac{2}{3}(n_d^2-1)\Delta G(\Delta)\right\} \tag{16}$$

where $R_{dc}=n_sR_c$ is the DC resistance of the slot conductor.

This shows that the resistance is smallest at the bottom layer and largest at the top layer. This means that in the case of series-connected conductors, the bottommost conductor contributes less to the resistive losses than the topmost conductor.

B. Saturation Factor

In the case of the conductor surrounded by a ferromagnetic material, the eddy current effect more remarkably occurs because much of the flux induced by the alternating current passes through the dense ferromagnetic material. Therefore, this phenomenon varies with the degree of magnetic saturation. First, consider the case shown in Fig. 3, where several

TABLE I
SPECIFICATIONS FOR THE COMPARISON OF LINEAR AND NONLINEAR ANALYSES

Parameter	Value
Conductor size	2.05x2.05 mm^2
Turn	400 turns
Air gap	0.5 mm
Stacking length	1,000 mm
Input current	1-10 Arms
Input frequency	10,000 Hz

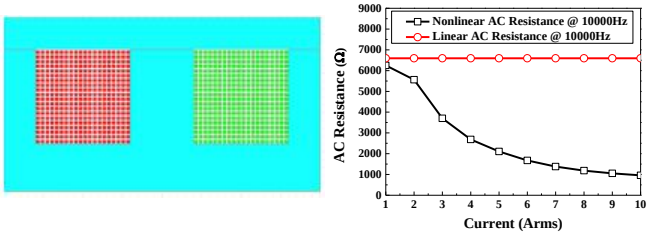

Fig. 3. Comparison of the linear and nonlinear analyses.

conductors are placed on a slot. Both linear and nonlinear analyses were done, as shown in Table 1.

In the case of the nonlinear analysis, it showed that the copper loss and AC resistance was decreased by the magnetic saturation of the core. Therefore, the saturation effect of the core has to be considered. The saturation factor, which is the ratio of the linkage flux of the linear and nonlinear analyses, is as follows:

$$\kappa_{sat} = \phi_{Non-linear} / \phi_{Linear} \tag{17}$$

When the skin effect is generated to the conductor, the effective section area of the conductor has to be considered. Thus, the resistance of the effective section area of the conductor is

$$R_{ac} = \frac{l}{\sigma S(\delta)} = \frac{l}{\pi\left(\frac{2a}{\sqrt{\pi f \mu}}\sqrt{\sigma} - \frac{1}{\pi f \mu}\right)} \tag{18}$$

where $S(\delta) = \pi a^2 - \pi(a-\delta)^2$ is the effective section area of the conductor and a is the radius of the conductor. The saturation factor was considered for the denominator term of equation (18), and it was included in the conductivity term of the conductor.

$$R'_{ac} = \frac{l}{\kappa_m^2 \cdot \pi\left(\frac{2a}{\sqrt{\pi f \mu}}\sqrt{\sigma} - \frac{1}{\pi f \mu}\right)} = \frac{l}{\pi\left(\frac{2a}{\sqrt{\pi f \mu}}\sqrt{\sigma'} - \frac{1}{\pi f \mu}\right)} \tag{19}$$

from which

$$\sigma' = [\kappa_m^2 \cdot \sqrt{\sigma} + \frac{1}{2a\sqrt{\pi f \mu}}(1-\kappa_m^2)]^2 \tag{20}$$

TABLE II
SPECIFICATIONS FOR THE COMPARISON OF THE FEM, TEST RESULT AND FORMULA

Parameter	Value
Conductor size	2.6x3.5 mm^2
Turn	24 turns
Air gap	1.0 mm
Stacking length	50 mm
Input current	2-32 Arms
Input frequency	50-500 Hz

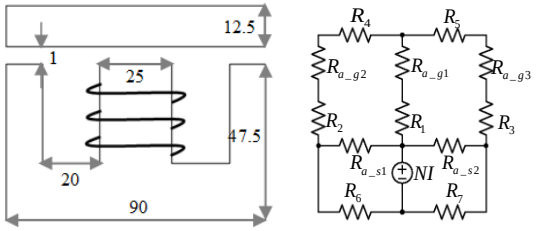

Fig. 4. EI core and equivalent circuit.

By substituting equation (20) into the skin effect term as shown in equation (21), and by solving equations (22) and (23), the AC resistance can be obtained considering the magnetic saturation in equation (23).

$$\delta' = \sqrt{2/\sigma'\mu\omega}\,,\ \nabla' = h/\delta' \tag{21}$$

$$F(\Delta') = \frac{\sinh 2\Delta' + \sin 2\Delta'}{\cosh 2\Delta' - \cos 2\Delta'},\ G(\Delta') = \frac{\sinh \Delta' - \sin \Delta'}{\cosh \Delta' + \cos \Delta'}, \text{ and} \tag{22}$$

$$R'_{AC} = R_{dc}\left\{\Delta' F(\Delta') + \frac{2}{3}(n_d^2 - 1)\Delta' G(\Delta')\right\} \tag{23}$$

where ' denotes the parameter considering the magnetic saturation. Therefore, the AC resistance increases as one moves from the slot bottom (n=1) to the slop top (n=n_d). Thus, more heat is generated at the slop top, where it is most difficult to remove, and it decreases when the saturation is increased.

III. EXPERIMENTAL VERIFICATION

A. EI Core Modeling

The EI core, which is identical to the motor shape, was modeled to verify the reliability of the analytical equation, and was experimented on. Also, only the portion of the motor was modelled for time saving, as shown in Fig. 5.

First, the relative permeability of the core was estimated using the numerical analysis approach . Next, the input current and frequency within the power supply limit in the process of equation (25) can be decided. Here, the leakage magnetic reluctances $\mathcal{R}_{a\_g1}$ and $\mathcal{R}_{a\_g2}$ are ignored.

$$\Re_{total} = \Re_1 + \Re_{a\_g1} + \left(\left(\Re_2 + \Re_4 + \Re_6 + \Re_{a\_g2}\right) \| \left(\Re_3 + \Re_5 + \Re_7 + \Re_{a\_g3}\right)\right) \tag{24}$$

Fig. 5. Test model and experimental equipment

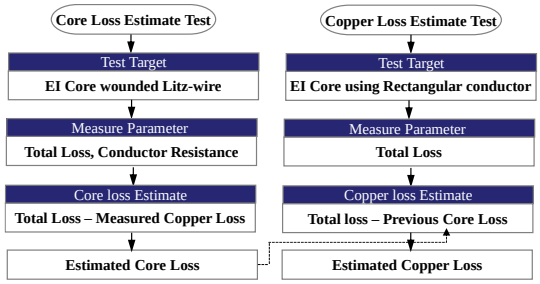

Fig. 6. Experiment process diagram

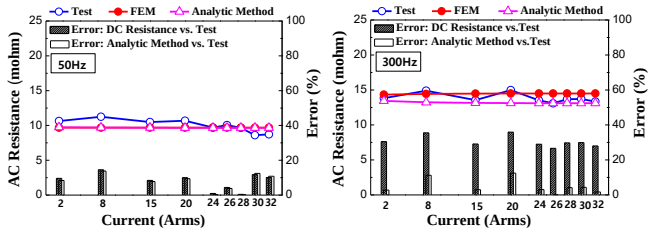

Fig. 7. AC resistance according to current at 50 and 300 Hz

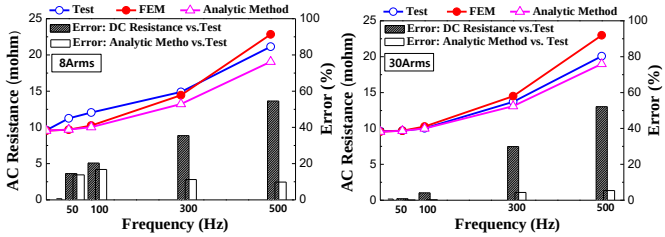

Fig. 8. AC resistance according to frequency at 8 and 30 Arms

$$L = \frac{N^2}{\Re_{total}}, \quad |Z| = |R + j\omega L|, \quad V_{input} = I_{input} \cdot Z \tag{25}$$

where N is the number of turns, $\mathscr{R}$ is the reluctance, Z is the impedance, R is the conductor resistance, ω is the frequency of excitation in radians per second, V is the input voltage, and I is the input current.

B. *Experiment Process*

The EI core was manufactured for comparison with the simulation result analyzed in section 3. It shows the test model and the experimental equipment shown in Fig. 6. The specifications are shown in Table II. The test was progressed according to the input frequency and current. The test must exclude the core loss from the measured loss to obtain the accurate AC resistance [5]. Thus, each test was progressed using two methods.

Firstly, the EI core wounded on a Litz wire was experimented on to separate the core loss. The Litz wire is designed to reduce the eddy current effect. In this step, the core loss can be estimated by excluding the copper loss from the total loss. Thereafter, the EI core wound on a rectangular conductor was experimented on under identical conditions. Therefore, the copper loss can be calculated by excluding the previously estimated core loss from the total loss. Finally, the AC resistance can be calculated with temperature correction. The test process diagram is shown in Fig. 7.

First, the results of the AC resistance at the 50 and 300 Hz currents were analyzed, as shown in Fig. 7. The AC resistance at 300 Hz was overall higher than the AC resistance at 50 Hz by about 40%. It is well known that the eddy current effect is intensified by increasing the frequency. In comparison, considering the error between the DC resistance and formula vs. the test result, the result of the presented formula is much more similar to the test result. Second, the frequency results of the AC resistance at 8 and 30 Arms were analyzed, as shown in Fig. 8. The AC resistance at 8 Arms was higher than the AC resistance at 30 Arms by about 12%. The eddy current effect slackened because the variation of the flux in the core was decreased by the magnetic saturation.

As a result, in the low-current section, which did not generate saturation, and the high-frequency section, which generated skin effect overlap, the AC resistance was highest at 300 Hz, as shown in Fig. 8 [6].

IV. Conclusion

This paper presents the saturation factor to consider the magnetic saturation of the core, and it complemented the existing equation. Also, the EI core, which is equivalent to the motor shape, was manufactured and experimented on as shown in the experiment process diagram to separate the core loss. As a result of the test, the experimental, simulation, and analytical results showed identical tendencies. Therefore, in the design of the motor, a more accurate prediction of the loss is possible using the presented equation.

ACKNOWLEDGMENT

This research was supported by the MSIP (Ministry of Science, ICT&Future Planning), Korea, under the CITRC (Convergence Information Technology Re-search Center) support program (NIPA-2013-H0401-13-1008) supervised by the NIPA (National IT Industry Promotion Agency).

References

[1] S.O. Kwon, S. I. Kim, P. Zhang, and J.P. Hong, "Performance comparison of IPMSM with distributed and concentrated windings" *IEEE Ind. Applications Conference*, Oct. 2006

[2] S. J. Lee, S. I. Kim, and J.P. Hong "Investigation on Core Loss according to Stator Shape in Interior Permanent Magnet Synchronous Motor" *International Con. on Elec. Mach. and System*, Oct. 2008

[3] J. Pyrhonen, T. Jokinen, and Valeria Hrabovcova,, *Design of Rotating Electrical Machines*, John Wiley & Sons, Ltd, 1, p256-260, 2008.

[4] D.C Hanselman, W.H Peake, "Eddy-current effects in slot-bound conductors", *IEE Proc.-Electr. Power Appl.*, Vol. 142,No.2,March 1995

[5] B. H. Lee, S. O. Kwon, T. Sun., and J. P. Hong, "Modeling of Core Loss Resistance for d-q Equivalent Circuit Analysis of IPMSM considering Harmonic Linkage Flux" *IEEE Trans. Magn.*, vol. 42, no. 5, May. 2011

[6] D. A. Gonzalez and D. M. Saban "Study of the Copper Losses in a High-Speed Permanent-Magnet Machine with Form-Wound Windings" *IEEE Trans. Ind. Electron.*, vol. 61, no. 6, June 2014